

Supplementary Information

**Trap-Limited Charge Recombination in Intrinsic Perovskite Film and Meso-
Superstructured Perovskite Solar Cells and the Passivation Effect of Hole-
Transport Material on Trap States**

Yi Wang, Hao-Yi Wang, Man Yu, Li-Min Fu, Yujun Qin^{a)}, Jian-Ping Zhang and Xi-Cheng Ai^{b)}
Department of Chemistry, Renmin University of China, Beijing 100872, P. R. China

S1. Preparation of intrinsic perovskite film

The perovskite film was fabricated on quartz substrate by means of one-step method for spectroscopy measurement. Firstly, the quartz substrate was washed successively with detergent, deionized water, acetone and isopropanol with 10 minutes and was then treated with the plasma cleaning. Next, PbCl₂ and CH₃NH₃I were mixed in DMF, respectively, with the concentration of 0.73 M and 2.2 M. After overnight stir, the mixed solution was spin-coated on the quartz substrates (2000 rpm, 30 seconds). Subsequently, the prepared film was thermally annealed at 100 °C for 1 h.

S2. Measurements of steady and transient absorption spectroscopy

Steady absorption spectra were recorded on a UV-3600 (Shimadzu) absorption spectrometer. For the measurement of transient absorption spectroscopy, an optical parametric amplifier (OPA-800 CF-1, Spectra Physics) pumped by a regenerative amplifier (SPTF-100F-1KHPR, Spectra Physics) provided the actinic laser pulses at desired wavelengths (~120 fs, full width at halfmaximum, 788 nm, 70). A white light continuum probe was generated from 1 cm thick water and was detected after interrogating the excited sample by a CCD detector (Spec-10:400B/LN) for the visible region. To ensure that each laser shot excites the sample relaxed fully from the previous excitation, the laser system was run at a repetition rate of 50 Hz. A mechanical chopper (model 75158, Newport) was set in the pump beam to regulate pump “on” and “off” for a pair of sequential actinic pulses. To improve the signal-to-noise ratio, each transient spectrum was obtained by averaging 200 individual measurements, and the typical detection sensitivity of the difference absorption (ΔOD) was better than 10^{-4} . The time-resolved absorption spectra were corrected against group velocity dispersion. All measurements were carried out at room temperature (296 K).

S3. Derivation of temporal evolution of electron density in trap-free and trap-limited recombination

It's well known that electron density is always determined from two aspects, i.e. distribution of electronic states and population probability of electrons while the latter is expressed by the Fermi-Dirac function. Therefore, the density of electrons in conduction band (n_c) can be written as:

$$n_c = N_c \exp\left(\frac{E_F - E_c}{k_B T}\right), \quad (\text{S1})$$

where N_c is the effective electronic states in conduction band, k_B is Boltzmann constant, T is temperature, E_F is Fermi level and E_c is the energy level of conduction band edge. Here we note that the Boltzmann approximation of Fermi-Dirac function is adopted. For the case of electrons in trap states, we performed the absolute-zero approximation for electron population [S1, S2] and give the expression of electron density in trap states (n_t) as:

$$n_t = \int_{-\infty}^{E_F} g_t(E) dE, \quad (\text{S2})$$

where $g_t(E)$ is the function of density-of-states (DOS) distribution. In the present work, DOS distribution was confirmed to be exponential (Figure 4b in main text), hence $g_t(E)$ can be written by: [S3]

$$g_t(E) = \frac{N_t}{k_B T_0} \exp\left(\frac{E - E_c}{k_B T_0}\right), \quad (\text{S3})$$

in which N_t is the total density of trap states and T_0 is the characteristic temperature of DOS distribution. Combining eq. (S2) with eq. (S3), one can obtain the expression of n_t as:

$$n_t = N_t \exp\left(\frac{E_F - E_c}{k_B T_0}\right), \quad (\text{S4})$$

Now let's consider the theoretical expression of recombination dynamics. For the photovoltaic system involving intra-gap trap states and within the multiple-trapping mechanism, time constant of charge recombination (τ_n) is generally written by [S4]:

$$\tau_n = -\ln X \frac{1}{\nu_0} \exp\left(\frac{E_c - E_F}{k_B T}\right), \quad (\text{S5})$$

where ν_0 is the attempt-to-jump frequency, X is a random number between 0 and 1. Meanwhile, τ_n can be also directly written by:

$$\frac{dn}{dt} = -\tau_n^{-1} n, \quad (\text{S6})$$

in which n is density of electrons involved in charge recombination and t is time.

In the case of trap-free recombination, the temporal evolution of electron density is obtain by combining eq. (S1), eq. (S5) with eq. (S6) and assuming $n = n_c$ which is given by

$$n_c = n_{c0} \left(1 - \frac{\nu_0}{\ln X} n_{c0} N_c^{-1} t\right)^{-1}, \quad (\text{S7})$$

where n_{c0} is the original density of electrons in conduction band.

Similarity, in the case of trap-limited recombination, the temporal evolution of electron density is obtain by combining eq. (S4), eq. (S5) with eq. (S6) and assuming $n = n_t$ which is given by

$$n_t = n_{t0} \left(1 - \frac{T_0 \nu_0}{T \ln X} n_{t0} \frac{T_0}{T} N_t^{-1} t\right)^{\frac{T}{T_0}}, \quad (\text{S8})$$

where n_{t0} is the original density of electrons in trap states.

Based on eq. (S7) and eq. (S8), the general expression of n - t relation is obtained as following:

$$n = n_0 (1 + at)^{-\alpha}, \quad (\text{S9})$$

in which n_0 , a and α are constants.

In details, for trap-free recombination,

$$n_0 = n_{c0}, \quad a = -\frac{v_0}{\ln X} n_{c0} N_c^{-1}, \quad \alpha = 1, \quad (\text{S10})$$

while for trap-limited recombination,

$$n_0 = n_{t0}, \quad a = -\frac{T_0 v_0}{T \ln X} n_{t0}^{\frac{T_0}{T}} N_t^{-\frac{T_0}{T}}, \quad \alpha = T / T_0, \quad (\text{S11})$$

as a result, $\alpha=1$ for trap-free recombination while $\alpha<1$ (because of $T<T_0$) for trap-limited recombination.

Importantly, it should be noted that when $\alpha=1$ we could easily derive the following equation from eq. (S9) and eq. (S10), that is

$$\frac{dn}{dt} = -\frac{a}{n_0} n^2, \quad (\text{S12})$$

which implies that trap-free recombination obeys the second-order kinetics.

S4. Kinetics of PA and PB2 with low exciting intensity

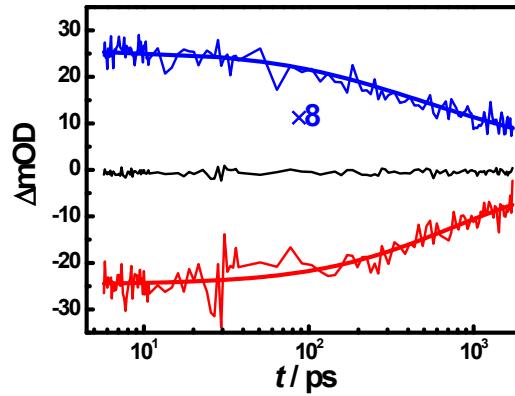


Figure S1. Kinetics of PB1 (black), PB2 (red) recoveries and PA decay (blue). The thin curves are experimental data while the thick curves denote the fitting results based on trap-free or trap-limited recombination models. Note that the signal of PB1 is lower than the noisy level, so it's unable to be accurately fitted.

Transient absorption spectroscopy with low exciting intensity ($20 \mu\text{J}/\text{cm}^2$ per pulse) was conducted. The kinetics PB2 recovery and PA decay are extracted out, as seen in Figure S1, which are fitted by the derived power functions, respectively, with $\alpha=1$ and $\alpha=0.5$. These results are same with that obtained under high exciting density as shown by Figure 2 in main text, i.e. the PB2 recovery and PA decay respectively reflect the trap-free and trap-limited recombination processes.

S5. Preparation of meso-superstructured perovskite solar cells

Three kinds of meso-superstructured perovskite solar cells were prepared following the

reported method. [S5] In briefly, the laser etched FTO glass substrates were washed for 10 min successively with detergent, deionized water, acetone and ethanol. Then the cleaned substrates were further treated with ozone plasma cleaner for 30 min to get rid of organic residues. Following the preparation of a compact TiO₂ hole blocking layer on FTO substrate, a diluted commercial paste was spin-coated on to form the mesoporous TiO₂ electrode. After gradually sintering to 550 °C for 15 min, the substrate was then dipped into a TiCl₄ (50 mM) aqueous solution for 15 min at 90 °C, and sintered at 500 °C for 30 min. Afterwards, the perovskite films were prepared by the modified sequential deposition method: firstly, DMF solution of PbI₂ (1 M) was dropped on the mesoporous TiO₂ scaffold and spun with a speed of 3000 rpm for 20s which was followed by the annealing at 100 °C for 15 min and cooling down to room temperature; secondly, the solution of CH₃NH₃I in isopropanol (0.044 M) was dropped on and spun with a speed of 4000 rpm for 20s. As thus, the perovskite film was prepared which allowed the succedent fabrication of HTM layer. It's noteworthy that among the three target samples all the components were strictly fabricated by the same craft as mentioned above, except for the layer of HTM. In details, the spin rate of HTM preparations are respectively 4000 rpm 20 s, 1000 rpm 8 s followed by 4000 rpm 20 s and 500 rpm 8 s followed by 4000 rpm 20 s. As a consequence, the thicknesses of HTM layers are distinctly different. The composition of HTM was 72.3 mg spiro-MeOTAD (2,2',7,7'-tetrakis-(N,N-di-p-methoxyphenylamine)-9,9'-spirobifluorene) with 28.8 μL TBP (4-tert-butylpyridine) and 17.5 μL of 520 mg/ml Li-TFSI (lithium bis(trifluoromethylsulphonyl)imide) in 1 ml chlorobenzene. Finally, 60 nm of Au was deposited by thermal evaporation.

S6. Current density-voltage (J-V) characterizations and SEM measurement for meso-superstructured perovskite solar cells

For photovoltaic performance characterization, the *J-V* curves were recorded by the solar simulator (Zolix SS150 solar simulator) with a source-meter (Keithley 2400) under illumination (100 mA/cm², AM 1.5G). The bias voltage ranges from -1.1V to 0.3V with a voltage step of 10 mV.

The SEM characterization was conducted using a JEOL JSM-7401F scanning electron microscope at an accelerating voltage of 5 kV with ~7 mm working distance and 10000-folds magnification.

S7. Experimental method of TRCE and OCVD measurements

TRCE measurements were conducted by the self-made apparatus which is seen in previous reports for details. [S6] By the utilization of a fast switch unit (temporal resolution: ~10 ns) which was connected in parallel with the perovskite solar cell, the experimental system could be quickly switched from open- to short-circuit at desired timing within the decay of photovoltage, as thus the kinetics of charge extraction can be obtained. By integrating these kinetics curves versus time, the temporal or voltage dependent charge amount could be obtained.

For OCVD measurement, the target cell was connected with the oscilloscope (output resistance: 1 MΩ) in open circuit. A pulse laser (wavelength: 532 nm, pulse width: 7 ns) irradiated the cell from FTO side to generate the photovoltage and the rise and decay traces of photovoltage were recorded by the oscilloscope.

S8. Kinetics of OCVD for meso-superstructured perovskite solar cells

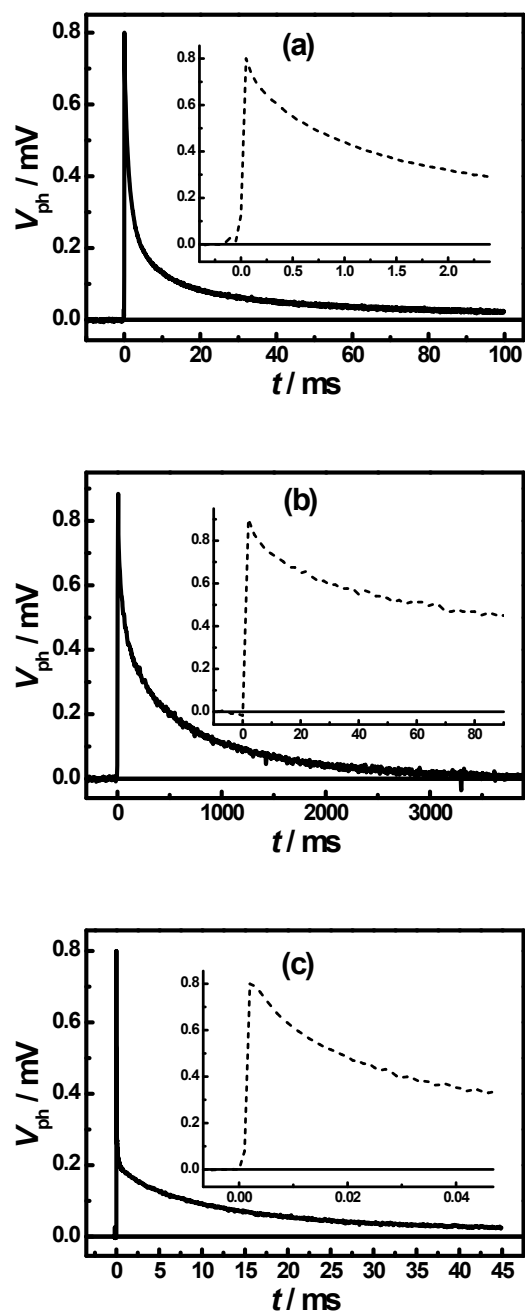


Figure S2. OCVD kinetics of cell-1 (a), cell-2 (b) and cell-3 (c). The insets are corresponding blow-ups to see the rise kinetics of V_{ph} .

REFERENCES

[S1] Bisquert, J.; Zaban, A.; Greenshtein, M.; Seró, I. M. *J. Am. Chem. Soc.*, 2004, **126**, 13550.

[S2] Wang, Y.; Wu, D. P.; Fu, L.-M.; Ai, X.-C.; Xu, D. S.; Zhang, J.-P. *Phys. Chem. Chem. Phys.* 2014, **16**, 11626.

[S3] Marshall, J. M. *Rep. Prog. Phys.* 1983, **46**, 1235.

[S4] Nelson, J. *Phys. Rev. B* **67**, 155209 (2003).

[S5] Im, J.-H.; Jang, I.-H.; Pellet, N.; Grätzel, M.; Park, N.-G. *Nature Nanotech.* 2014, **9**, 927.

[S6] Wang, Y.; Wu, D. P.; Fu, L.-M.; Ai, X.-C.; Xu, D. S.; Zhang, J.-P. *ChemPhysChem* 2015, **16**, 2253-2259.